Formation of a heteronuclear hydrolysis complex in the Th^{IV}/Fe^{III} system

Natallia Torapava,[a] Artsiom Radkevich,[b] Ingmar Persson,[a*] Dmitri Davydov[b] and Lars Eriksson[c]

Electronic Supplementary Information

Figure S1. XRD patterns for A-3.5 after increasing pH to about 12.

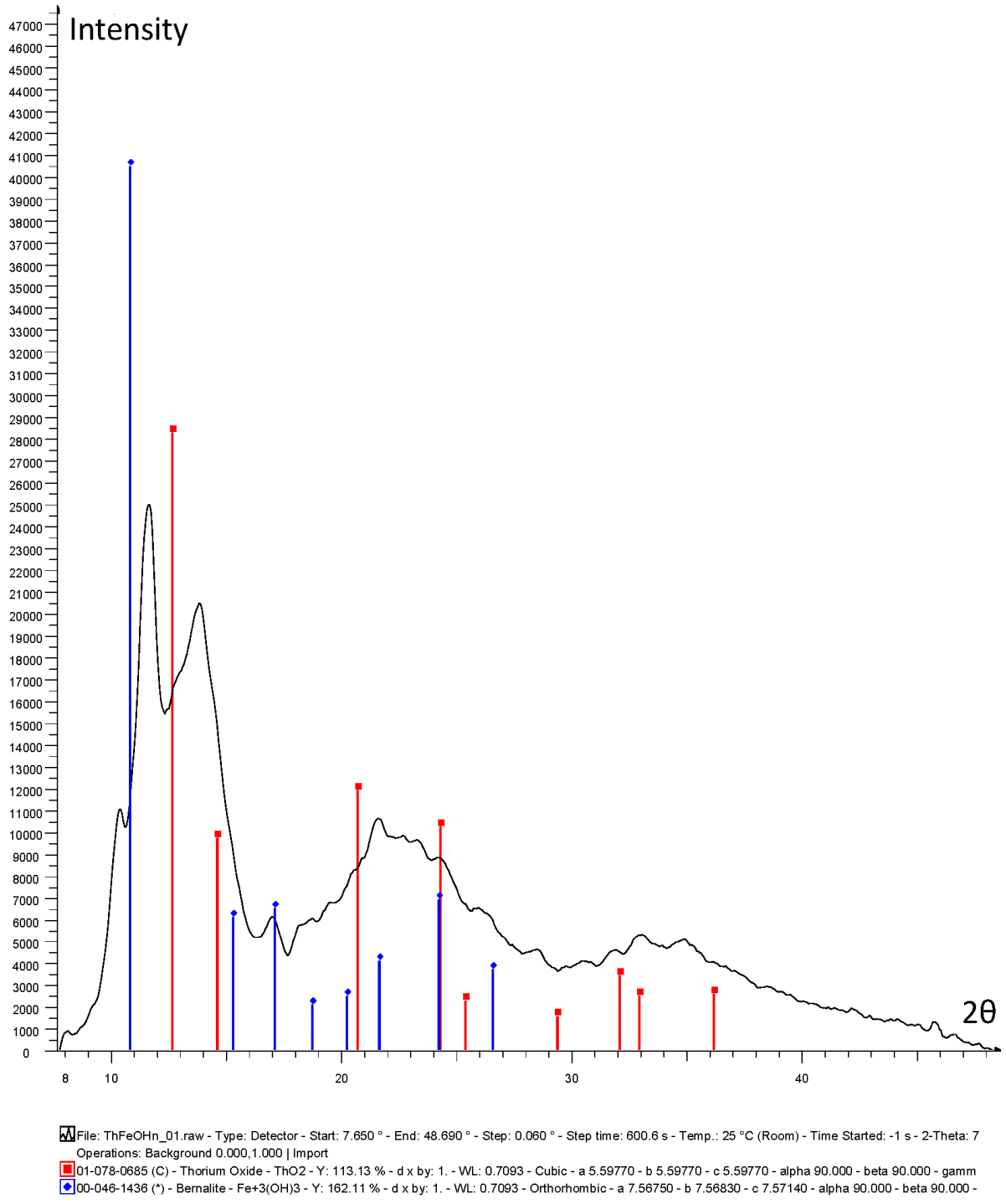

Figure S2. Diagram of thorium(IV) species distribution at $C_{Th} = 1 \cdot 10^{-2}$ mol·cm^{-3} at different pH values (α – part of thorium(IV) present as polynuclear species) .

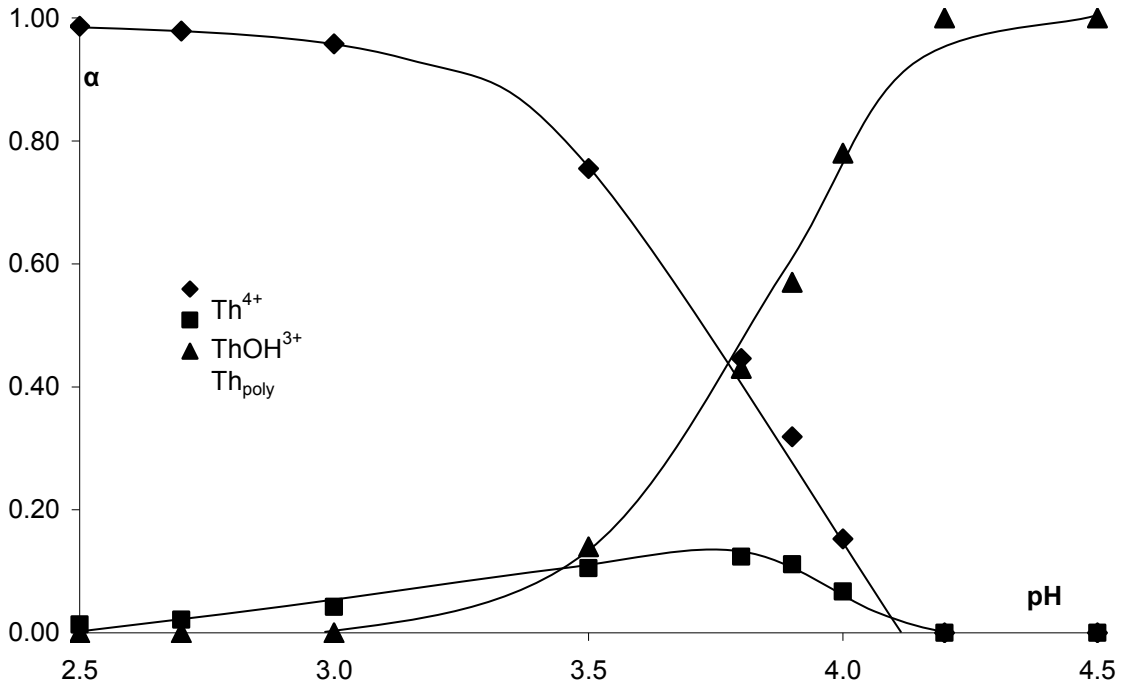

Figure S3a. Fit and the individual contribution of the different scattering paths of the Fe K edge EXAFS data of solution A-2.9, thin line – experimental data, thick line - calculated model function using the parameters given in Table 2, and the individual contributions of single scattering Fe-O (offset -6), multiple scattering within FeO_6 (offsets -10, -12 and -14), single scattering Fe···Fe (offset -16), and single scattering Fe···Th (offset -18).

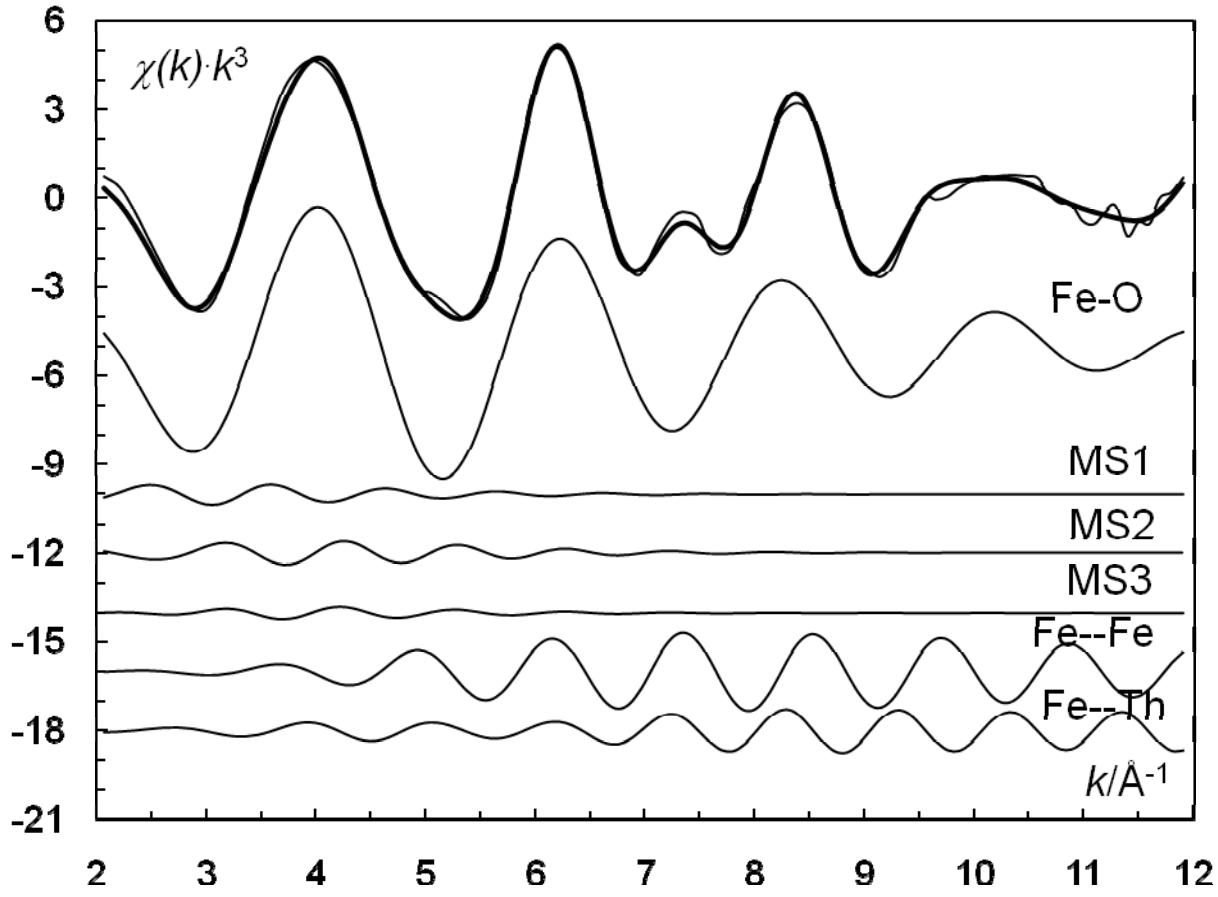

Figure S3b. Fit and the individual contribution of the different scattering paths of the Fe K edge EXAFS data of solution C-2.9, thin line – experimental data, thick line - calculated model function using the parameters given in Table 2, and the individual contributions of single scattering Fe-O (offset -6), multiple scattering within FeO_6 (offsets -10, -12 and -14), single scattering Fe···Fe (offset -16), and single scattering Fe···Th (offset -18).

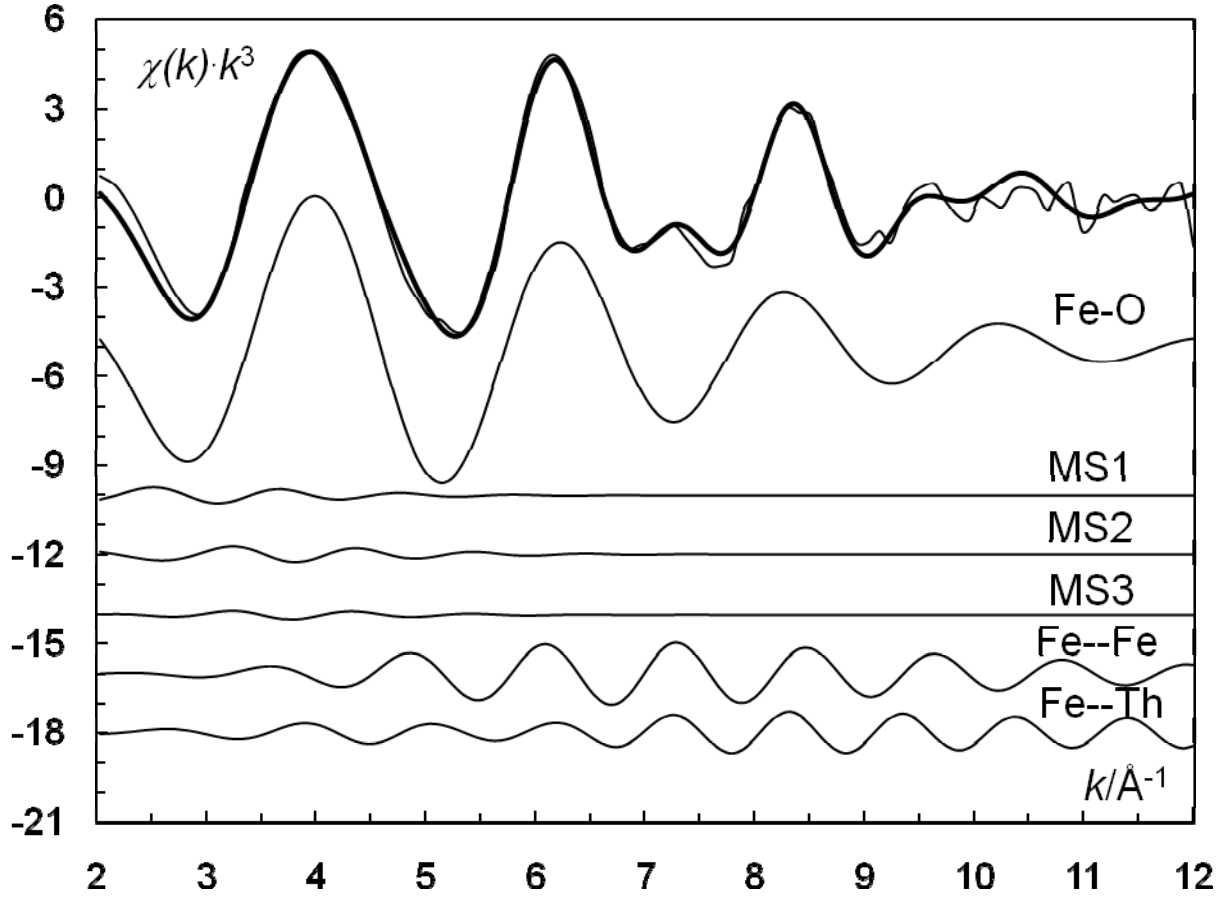

Figure S3c. Fit and the individual contribution of the different scattering paths of the Th L_3 edge EXAFS data of solution A-2.9, thin line – experimental data, thick line - calculated model function using the parameters given in Table 2, and the individual contributions of single scattering Th-O (offset -4), single scattering Th···Th (offset -8) and single scattering Th···Fe (offset -10).

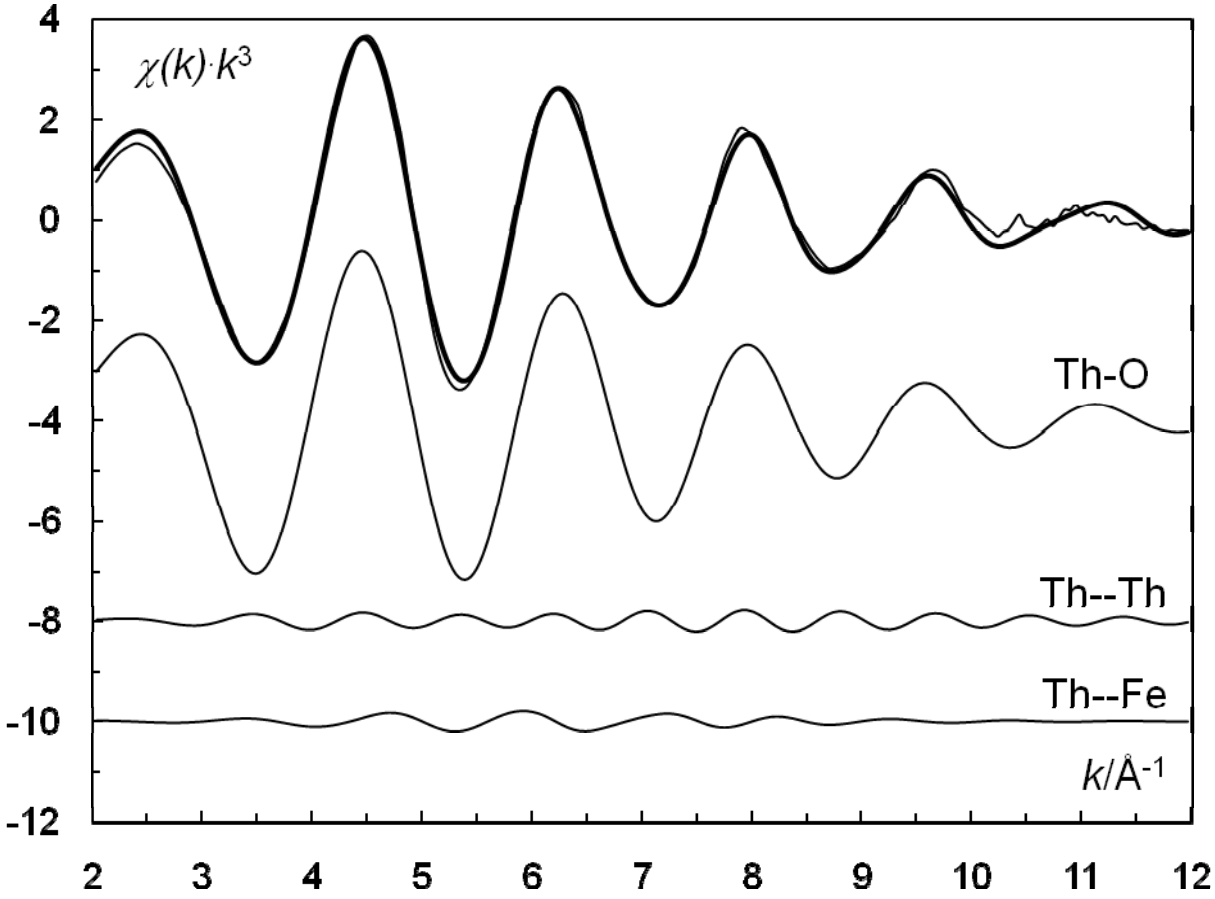

Figure S3d. Fit and the individual contribution of the different scattering paths of the Th L_3 edge EXAFS data of solution C-2.9, thin line – experimental data, thick line - calculated model function using the parameters given in Table 2, and the individual contributions of single scattering Th-O (offset -4), single scattering Th···Th (offset -8), single scattering Th···Fe_1 (offset -10), and single scattering Th···Fe_2 (offset -12).

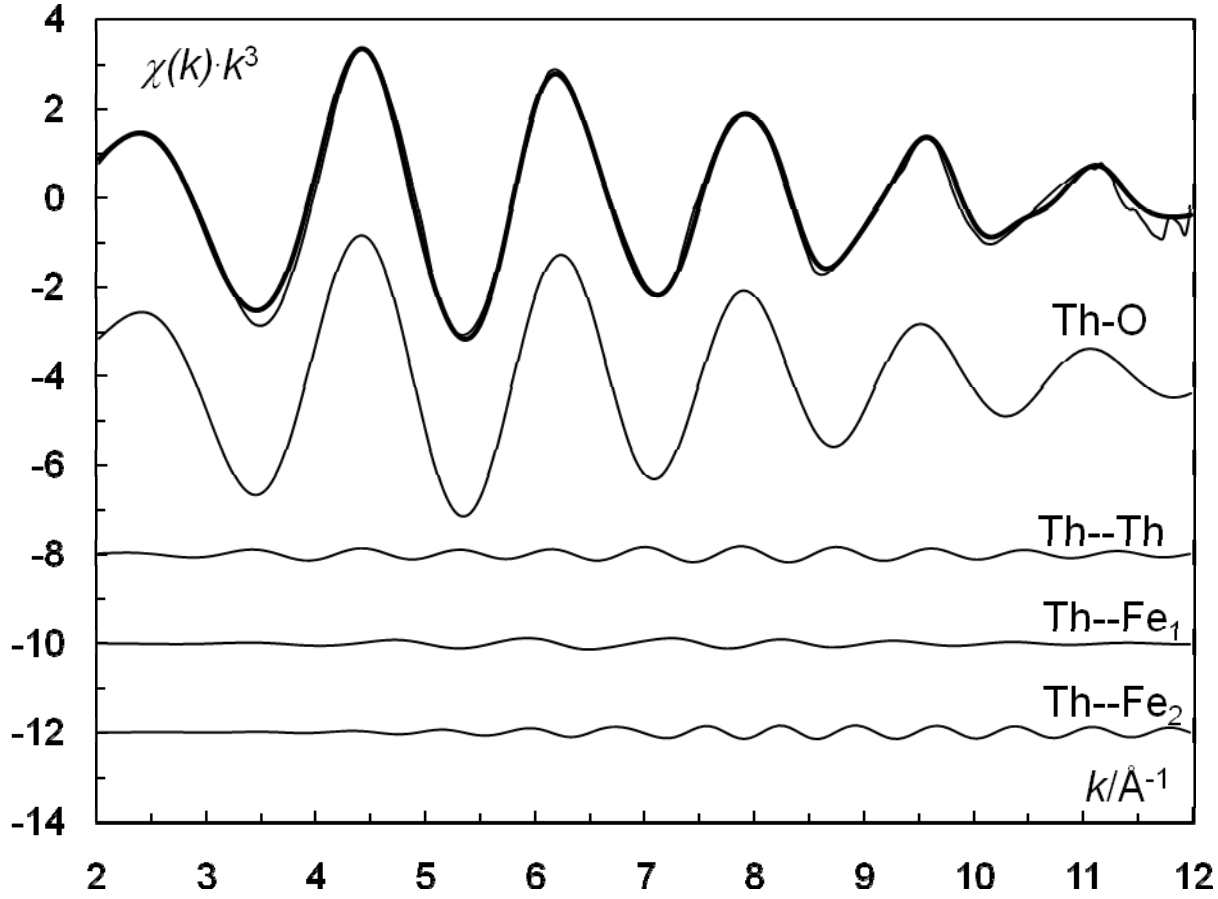

Figure S4. UV-visible spectra of Th^{IV}/Fe^{III} solutions, series A.